6774–6784 *Nucleic Acids Research, 2010, Vol. 38, No. 19* *Published online 27 May 2010*
doi:10.1093/nar/gkq458

Synthesis and characterization of oligodeoxyribonucleotides containing a site-specifically incorporated N^6-carboxymethyl-2′-deoxyadenosine or N^4-carboxymethyl-2′-deoxycytidine

Jianshuang Wang and Yinsheng Wang*

Department of Chemistry, University of California, Riverside, CA 92521-0403, USA

Received April 14, 2010; Revised May 8, 2010; Accepted May 10, 2010

ABSTRACT

Humans are exposed to both endogenous and exogenous *N*-nitroso compounds (NOCs), and many NOCs can be metabolically activated to generate a highly reactive species, diazoacetate, which is capable of inducing carboxymethylation of nucleobases in DNA. Here we report, for the first time, the chemical syntheses of authentic N^6-carboxymethyl-2′-deoxyadenosine (N^6-CMdA) and N^4-carboxymethyl-2′-deoxycytidine (N^4-CMdC), liquid chromatography–ESI tandem MS confirmation of their formation in calf thymus DNA upon diazoacetate exposure, and the preparation of oligodeoxyribonucleotides containing a site-specifically incorporated N^6-CMdA or N^4-CMdC. Additionally, thermodynamic studies showed that the substitutions of a dA with N^6-CMdA and dC with N^4-CMdC in a 12-mer duplex increased Gibbs free energy for duplex formation at 25°C by 5.3 and 6.8 kcal/mol, respectively. Moreover, primer extension assay revealed that N^4-CMdC was a stronger blockade to Klenow fragment-mediated primer extension than N^6-CMdA. The polymerase displayed substantial frequency of misincorporation of dAMP opposite N^6-CMdA and, to a lesser extent, misinsertion of dAMP and dTMP opposite N^4-CMdC. The formation and the mutagenic potential of N^6-CMdA and N^4-CMdC suggest that these lesions may bear important implications in the etiology of NOC-induced tumor development.

INTRODUCTION

Human genome is frequently attacked by various endogenous and exogenous species, and the resulting damage to DNA has been implicated in a number of pathological conditions including cancer and neurological disorders (1). Emerging data have supported a previous hypothesis that DNA damage induced by *N*-nitroso compounds (NOCs) in the gastric cavity may constitute the early steps of carcinogenesis in gastric cancer due to the high nitrite content of the gastric juice (2,3). In a recent review, Risch (4) proposed that frequent gastrointestinal exposure to NOCs contributes to increased risk of developing pancreatic cancer. In this respect, NOCs induce DNA adducts and single-strand breaks (5), which appear to stimulate DNA synthesis in the pancreatic ductal epithelium (6). Thus, exposure to NOCs may work synergistically with other factors to induce tumor development (7).

Humans are exposed to NOCs from diet, tobacco smoke and other environmental sources as well as from endogenous sources, and it was estimated that endogenous sources contribute to 45–75% of the total NOC exposure (3). Earlier studies by Wogan and colleagues (8) revealed that the treatment of male Fischer rats with nitrosated bile acid conjugates *N*-nitrosoglycocholic acid (NOGC) and *N*-nitrosotaurocholic acid (NOTC) could induce hepatocarcinoma in 54–70% of the treated animals and gastric tumors in 12–13% of the treated rats. Forward mutation assays showed that NOGC and NOTC are mutagenic in bacteria cells and human lymphoblasts. In this regard, NOGC could arise from the nitrosation of glycocholic acid under simulated gastric conditions (9,10). The treatment of calf thymus DNA with NOGC could induce the formation of O^6-carboxymethyl-2′-deoxyguanosine (O^6-CMdG) and,

*To whom correspondence should be addressed. Tel: 951 827 2700; Fax: 951 827 4713; Email: yinsheng.wang@ucr.edu

much less frequently, O^6-methyl-2′-deoxyguanosine (O^6-MdG) (11). By using immunoslot blot assay or immunoaffinity/HPLC method with antibody recognizing O^6-carboxymethylguanine, Shuker and coworkers (12–14) showed that O^6-CMdG could be induced in DNA by *N*-nitrosoglycine. In addition, *O*-diazoacetyl-L-serine (also known as azaserine), a pancreatic carcinogen (15), could result in the carboxymethylation of guanine residues in DNA of pancreatic acinar cells (16).

The NOC-induced DNA carboxymethylation was thought to occur through a common reactive intermediate, diazoacetate, which was shown to induce the formation of O^6-CMdG and, much less efficiently (about 1/16 of that of O^6-CMdG), O^6-MdG in DNA (12–14). In addition, the passage of potassium diazoacetate (KDA)-treated, human *p*53 gene-containing plasmid in yeast cells could lead to substantial single-base substitutions. Importantly, the mutation spectra of KDA obtained from the shuttle vector study exhibit remarkable similarity as the mutation spectra of *p*53 gene in human stomach and colorectal cancers (17). This finding underscores that gastrointestinal exposure to NOCs and the resulting generation of diazoacetate may constitute a significant etiological factor for the development of gastrointestinal tumors (17). In addition, KDA induced almost equal frequencies of transition and transversion mutations, which is distinctive from the predominant GC→AT transition mutation (>80%) induced by methylating agent methylnitrosourea (17). Moreover, the percentages of mutations occurring at AT base pairs contribute to 43 and 28% of all observed mutations, while the *p53* gene-containing vector was treated with KDA in PBS and Tris–EDTA, respectively. The above observation supports that KDA can induce promutagenic lesions at both GC and AT base pairs in DNA.

As discussed above, KDA was found to induce the formation of O^6-CMdG and we recently reported the formation of *N*3- and O^4-carboxymethylthymidine in calf thymus DNA upon exposure to KDA (18). However, it remains unexplored what type of DNA lesions can be induced at adenine and cytosine sites in DNA. In the present study, we set out to examine the chemistry of diazoacetate-induced modifications of adenine and cytosine in DNA, and to synthesize oligodeoxyribonucleotides (ODNs) containing carboxymethylated derivatives of 2′-deoxyadenosine and 2′-deoxycytidine at defined sites. In addition, we will have a preliminary assessment about how these lesions destabilize duplex DNA and how they perturb DNA replication *in vitro*.

MATERIALS AND METHODS

Materials

Chemicals and reagents were purchased from Sigma-Aldrich (St Louis, MO, USA) and Thermo Fisher Scientific (Pittsburgh, PA, USA) unless otherwise specified. Reagents for solid-phase DNA synthesis were obtained from Glen Research Co. (Sterling, VA, USA) and unmodified ODNs were from Integrated DNA Technologies (Coralville, IA, USA). Calf intestinal alkaline phosphatase and Klenow fragment (Kf$^-$) were purchased from US Biological (Swampscott, MA, USA) and New England Biolabs (Beverly, MA, USA), respectively. [$\gamma-^{32}$P]ATP was obtained from Amersham Biosciences Co. (Piscataway, NJ, USA).

Mass spectrometry and NMR

Electrospray ionization-mass spectrometry (ESI-MS) and tandem MS (MS/MS) experiments were carried out on an LCQ Deca XP ion-trap mass spectrometer (Thermo Fisher Scientific, San Jose, CA, USA). A mixture of methanol and water (50:50, v/v) was used as solvent for electrospray. The spray voltage was 3.0 kV, and the temperature of the heated capillary was maintained at 300°C. High-resolution mass spectra (HRMS) were acquired on an Agilent 6210-TOF LC/MS instrument (Agilent Technologies, Santa Clara, CA, USA) equipped with an ESI source. ^{1}H NMR spectra were recorded on Varian Inova NMR spectrometers at 300 or 400 MHz (Varian Inc., Palo Alto, CA, USA) and ^{31}P NMR spectra were acquired at 80 MHz. The $H_{2'}$ and $H_{2''}$ protons on nucleosides were assigned based on coupling constant measurements (19).

HPLC

HPLC experiments were performed on an Agilent 1100 HPLC System with an Apollo C18 column (4.6 × 250 mm, 5 μm in particle size and 300 Å in pore size; W. R. Grace & Co., Deerfield, IL, USA). For the purification of ODNs, a triethylammonium acetate buffer (50 mM, pH 6.6, Solution A) and a mixture (Solution B) of solution A and acetonitrile (70/30, v/v) were employed as mobile phases. The flow rate was 0.8 ml/min and gradient profiles in terms of solution B were as following: (Gradient I) 5 min 0–20%, 40 min 20–40%, 15 min 40–100% and 5 min at 100%; (Gradient II) 5 min 0–35%, 60 min 35–50%, 10 min 50–100% and 10 min at 100%.

For the separation of nucleosides, an ammonium formate buffer (10 mM, pH 6.9, Solution A) and a mixture of Solution A and acetonitrile (70/30, v/v, Solution B) were served as mobile phases. The flow rate was 0.8 ml/min and Gradient III used in this experiment was 5 min 0–10 % Solution B followed by 40 min 10–40% Solution B.

LC–MS/MS

Coupled liquid chromatography–ESI tandem MS (LC–MS/MS) experiments were performed using an Agilent 1100 capillary HPLC pump and an LTQ linear ion trap mass spectrometer (Thermo Fisher Scientific, San Jose, CA, USA). A Zorbax SB-C18 column (0.5 × 150 mm, 5 μm in particle size; Agilent Technologies) was used, and a 0.1% formic acid in water (Solution A) and a 0.1% formic acid in methanol (Solution B) were employed as mobile phases. The ESI spray voltage was 3.0 kV, and the temperature for the heated capillary was maintained at 275°C.

Synthesis of N^6-ethoxycarbonylmethyl-2′-deoxyadenosine (1a)

Compound **1a** was synthesized according to previously published procedures for the preparation of other N^6-substituted 2′-deoxyadenosine derivatives (Scheme 1a) (20,21). Glycine ethyl ester was synthesized following previously published procedures (22,23). To a round bottom flask were added commercially available 6-chloro-9-(2-deoxy-β-D-erythro-pentofuranosyl)purine (6-CldA, 70 mg, 0.26 mmol; Berry & Associates, Dexter, MI, USA), glycine ethyl ester (132 mg, 1.3 mmol), triethylamine (TEA) (209 µl, 1.5 mmol) and anhydrous acetonitrile (5.0 ml). The solution was stirred at room temperature for 2 days and the solvent was removed *in vacuo*. Product **1a** was isolated by silica gel column chromatography with EtOAc and then EtOAc/MeOH (50/1, v/v) as mobile phases. The product was obtained in white solid (48 mg; yield: 61%). HRMS (ESI): $[M+H]^+$ calcd m/z 338.1464, found 338.1470. ^{1}H NMR (400 MHz, $CDCl_3$, 25°C; Supplementary Figure S1): δ 8.33 (s, 1H, H-8), 7.87 (s, 1H, H-2), 6.61 (broad, 1H, NH), 6.35 (t, 1H, H-1′, J = 6.4 Hz), 4.78 (m, 1H, H-3′), 4.41 (broad, 2H, 3′-OH and 5′-OH) 4.25 (m, 5H, H-4′, NCH_2 and OCH_2), 3.95 (m, 1H, H-5′), 3.81 (m, 1H, H-5″), 3.05 (m, 1H, H-2′), 2.33 (m, 1H, H-2″), 1.30 (t, 3H, CH_3, J = 6.0 Hz).

Synthesis of N^6-carboxymethyl-2′-deoxyadenosine (N^6-CMdA)

Compound **1a** (20 mg) was dissolved in 1.5 ml methanol and to the solution 1.0 M NaOH (1.5 ml) was added (Scheme 1a). The mixture was stirred at room temperature for 6 h to complete the hydrolysis of the ethyl ester in **1a**. The solution was then neutralized with 1.0 M HCl and the solvent was removed in a Speed-vac to afford light yellow solid that was washed with $CHCl_3$ (200 µl × 3) and extracted with methanol (500 µl × 4). The methanol layer was combined and dried to render N^6-CMdA as a pale yellow solid (16 mg; yield: 87%). HRMS (ESI): $[M+H]^+$ calcd m/z 310.1151, found 310.1159. ^{1}H NMR (400 MHz, D_2O, 25°C; Supplementary Figure S2): δ 8.15 (s, 1H, H-8), 8.06 (s, 1H, H-2), 6.33 (t, 1H, H-1′, J = 6.7 Hz), 4.55 (m, 1H, H-3′), 4.08 (s, 1H, H-4′), 3.96 (broad, 2H, NCH_2), 3.74 (m, 1H, H-5′), 3.68 (m, 1H, H-5″), 2.69 (m, 1H, H-2′), 2.49 (m, 2H, H-2″).

Synthesis of 3′,5′-*O*-diacetyl-N^4-ethoxycarbonylmethyl-2′-deoxycytidine (2b)

Compound **2b** was synthesized following previously reported procedures for syntheses of relevant uridine derivatives (Scheme 1b) (24,25). Compound **2a** (181 mg, 0.5 mmol), prepared following previously described protocols (26), glycine ethyl ester (102 mg, 1.0 mmol) and TEA (167 µl, 1.2 mmol) were mixed in anhydrous acetonitrile (10 ml) in a round bottom flask and the solution was stirred at room temperature for 3 days. The solvent was removed *in vacuo* and product **2b** was isolated by silica gel column chromatography by using EtOAc as mobile phase. The product was obtained as yellowish oil (95 mg; yield: 48%). HRMS (ESI): $[M+H]^+$ calcd m/z 398.1563, found 398.1571. ^{1}H NMR (300 MHz, $CDCl_3$, 25°C; Supplementary Figure S3): δ 7.66 (d, 1H, H-6, J = 6.0 Hz), 6.28 (t, 1H, H-1′, J = 6.4 Hz), 6.09 (broad, 1H, NH), 5.82 (d, 1H, H-5, J = 6.0 Hz), 5.17 (m, 1H, H-3′), 4.32 (m, 1H, H-4′), 4.20 (m, 6H, NCH_2, ethoxy CH_2, H-5′ and H-5″), 2.68 (m, 1H, H-2″), 2.00 (m, 2H, H-2′), 2.05 (s, 3H, acetyl CH_3), 2.06 (s, 3H, acetyl CH_3), 1.27 (s, 3H, CH_3).

Synthesis of N^4-carboxymethyl-2′-deoxycytidine (N^4-CMdC)

The method for the synthesis of N^6-CMdA was used with slight modification, where the hydrolysis of **2c** was carried

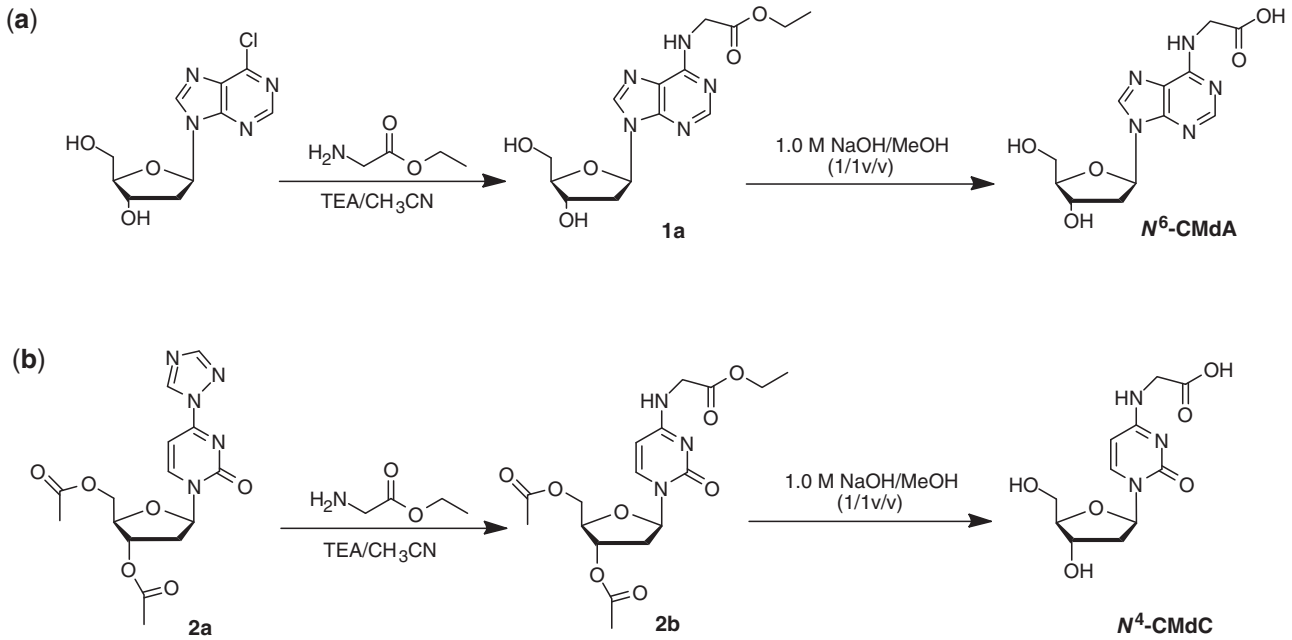

Scheme 1. Syntheses of authentic N^6-CMdA (**a**) and N^4-CMdC (**b**).

out for one day to complete the deprotection of two hydroxyl groups (Scheme 1b). N^4-CMdC was obtained as white solid (yield: 92%). HRMS (ESI): $[M+H]^+$ calcd m/z 286.1039, found 286.1045. ^{1}H NMR (300 MHz, D_2O, 25°C; Supplementary Figure S4): δ 7.79 (d, 1H, H-6, J = 6.0 Hz), 6.33 (t, 1H, H-1′, J = 6.7 Hz), 6.13 (d, 1H, H-5, J = 6.0 Hz), 4.48 (m, 1H, H-3′), 4.10 (m, 1H, H-4′), 3.86 (broad, 2H, NCH_2), 3.87–3.80 (m, 2H, H-5′ and H-5″), 2.50–2.30 (m, 2H, H-2″ and H-2′).

Synthesis of 5′-*O*-(4,4′-dimethoxytrityl)-N^6-ethoxycarbonylmethyl-2′-deoxyadenosine (1b)

Compound **1a** (60 mg) was dissolved in anhydrous pyridine (3.0 ml) and the solution was cooled in an ice bath. To the solution were added 4-dimethylaminopyridine (DMAP, 0.5 mg) and dimethoxytrityl chloride (DMTr-Cl, 72 mg), and the resulting solution was stirred at room temperature for 90 min (Scheme 2a). The reaction was then quenched with methanol (0.1 ml) and the solvent was removed under reduced pressure. The product was isolated from the reaction mixture on a silica gel column with the use of EtOAc as mobile phase. The product was obtained as yellow foam (88 mg; yield: 77%). HRMS (ESI): $[M+H]^+$ calcd m/z 640.2771, found 640.2783. ^{1}H NMR (400 MHz, DMSO-d_6, 25°C; Supplementary Figure S5): δ 8.29 (s, 1H, H-8), 8.15 (s, 1H, H-2), 7.32 (m, 5H, aromatic Hs), 7.21–7.19 (m, 5H, 4 aromatic Hs and NH), 6.81 (m, 4H, aromatic Hs), 6.38 (t, 1H, H-1′, J = 6.5 Hz), 5.36 (m, 1H, H-3′), 4.47 (broad, 1H, 3′-OH), 4.25–3.90 (m, 5H, H-4′, NCH_2 and ethoxy CH_2), 3.72 (s, 6H, OCH_3), 3.17 (m, 2H, H-5′and H-5″), 2.87 (m, 1H, H-2′), 2.33 (m, 1H, H-2″), 1.17 (t, 3H, CH_3, J = 6.2 Hz).

Synthesis of 5′-*O*-(4,4′-dimethoxytrityl)-N^6-ethoxycarbonylmethyl-2′-deoxyadenosine-3′-*O*-[(2-cyanoethyl)-*N*,*N*-diisopropylphosphoramidite] (1c)

To a round bottom flask, which was suspended in an ice bath and contained a solution of compound **1b** (80 mg) in dry CH_2Cl_2 (5.0 ml), was added *N*,*N*-diisopropylethylamine (DIEA, 50 µl) followed by 2-cyanoethyl-*N*,*N*-diisopropyl chlorophosphoramidite (48 µl) (Scheme 2a). The mixture was stirred at room temperature for 30 min under an argon atmosphere and quenched by adding 0.1 ml CH_3OH. The solution was then mixed quickly with

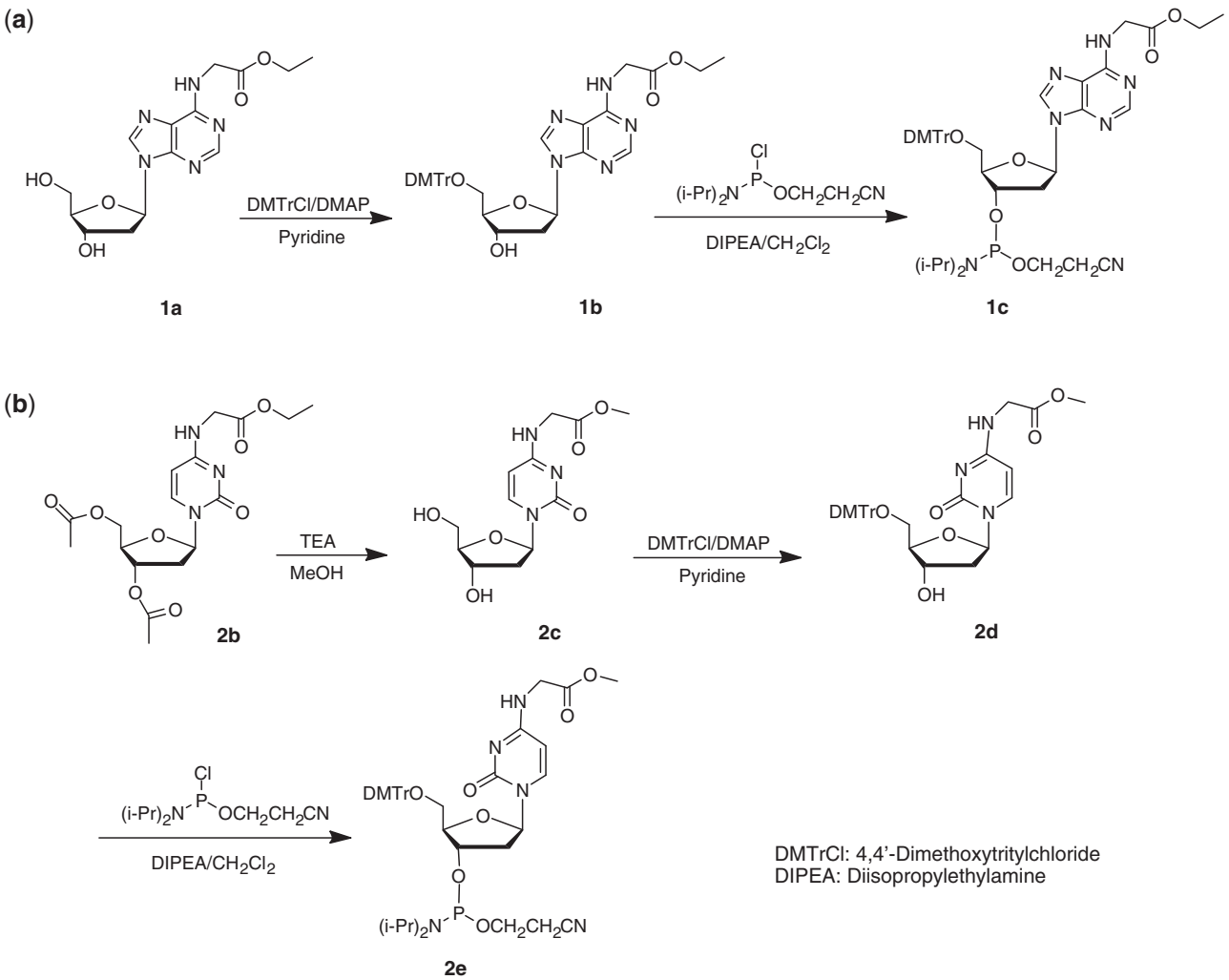

Scheme 2. Syntheses of phosphoramidite building blocks of ethyl ester derivative of the N^6-CMdA (**a**) and methyl ester derivative of N^4-CMdC (**b**).

EtOAc(8.0 ml). The organic phase was washed with saturated $NaHCO_3$ (2.0 ml), brine (2.0 ml) and dried with anhydrous Na_2SO_4. The solvent was evaporated under reduced pressure to yield final product **1c** in white foam, which was used directly for ODN synthesis (72 mg; yield; 68%). HRMS (ESI): $[M+Na]^+$ calcd m/z 862.3669, found 862.3678. ^{31}P NMR (80 MHz, $CDCl_3$, 25°C; Supplementary Figure S6): δ 149.8, 149.0.

Synthesis of N^4-methoxycarbonylmethyl-2′-deoxycytidine (2c)

Compound **2b** (95 mg) was dissolved in 3.0 ml of 0.4 M triethylamine in methanol and the solution was stirred at room temperature for 2 days (Scheme 2b) (25). The solution was concentrated to a small volume and co-evaporated with anhydrous methanol (twice) and toluene (twice) to give white solid (66 mg; yield: 92%). HRMS (ESI): $[M+H]^+$ calcd m/z 300.1196, found 300.1202. ^1H NMR (300 MHz, $CDCl_3$, 25°C; Supplementary Figure S7): δ 8.31 (s, 1H, NH), 7.97 (d, 1H, H-6, J = 6.0 Hz), 6.25 (t, 1H, H-1′, J = 7.0 Hz), 5.95 (d, 1H, H-5, J = 7.5 Hz), 4.86 (broad, 2H, 3′-OH and 5′-OH), 4.36 (m, 1H, H-3′), 4.17 (s, 2H, NCH_2), 3.93 (m, 1H, H-5′), 3.80–3.65 (m, 4H, OCH_3 and H-5″), 3.32 (m, 1H, H-4′), 2.34 (m, 1H, H-2″), 2.15 (m, 1H, H-2′).

Synthesis of 5′-*O*-(4,4′-dimethoxytrityl)-N^4-methoxycarbonylmethyl-2′-deoxycytidine (2d)

This compound was synthesized following the similar procedures as described for the synthesis of **1b** (Scheme 2b). For the purification of this compound, the silica gel column was first washed with CH_2Cl_2 (with 0.1% TEA) and the desired compound was eluted from the column with CH_2Cl_2/CH_3OH (9/1 with 0.1% TEA). Compound **2d** was obtained as yellow foam (yield: 74%). HRMS (ESI): $[M+H]^+$ calcd m/z 602.2502, found 602.2511. ^1H NMR (300 MHz, DMSO-d_6, 25°C; Supplementary Figure S8): δ 8.08 (m, 1H, NH), 7.67 (d, 1H, H-6, J = 6.3 Hz), 7.40–7.17 (m, 9H, aromatic Hs), 6.90 (m, 4H, aromatic Hs), 6.13 (t, 1H, H-1′, J = 6.7 Hz), 5.70 (d, 1H, H-5, J = 7.5 Hz), 5.26 (s, 1H, 3′-OH), 4.27 (m, 1H, H-3′), 4.13–4.06 (m, 2H, H-5′ and H-5″), 3.82 (m, 1H, H-4′), 3.75 (s, 3H, $COOCH_3$), 3.64 (s, 2H, NCH_2), 3.32 (m, 6H, OCH_3,), 2.20 (m, 1H, H-2″), 2.10 (m, 1H, H-2′).

Synthesis of 5′-*O*-(4,4′-dimethoxytrityl)-N^4-methoxycarbonylmethyl-2′-deoxycytidine-3′-*O*-[(2-cyanoethyl)-*N*,*N*-diisopropylphosphoramidite] (2e)

This compound was synthesized following the similar procedures as described for the synthesis of **1c** (Scheme 2b). Compound **2e** was obtained as white foam, which was used directly for ODN synthesis without further purification (yield: 75%). HRMS (ESI): $[M+Na]^+$ calcd m/z 824.3400, found 824.3413. ^{31}P NMR (80 MHz, $CDCl_3$, 25°C; Supplementary Figure S9): δ 150.1, 149.6.

KDA treatment of calf thymus DNA

KDA was prepared through alkaline hydrolysis of ethyl diazoacetate following previously described procedures (17,18) and its stock solution (0.8 M) was diluted to an appropriate concentration before usage. Calf thymus DNA (1.0 mg/ml) in PBS buffer (pH 7.3) was treated with freshly prepared KDA solution (10 mM) at 37°C overnight. The resulting DNA was desalted by ethanol precipitation and the recovered DNA pellets were then taken up in doubly distilled water and digested with four enzymes. One unit of nuclease P1, 0.01 U of calf spleen phosphodiesterase, and 2.5 μl of buffer solution containing sodium acetate (300 mM, pH 5.0) and zinc acetate (10 mM) were added to a 20 μl solution of KDA-treated calf thymus DNA (20 μg). The digestion was continued at 37°C for 6 h. To the digestion mixture were then added 10 U of alkaline phosphatase, 0.05 U of snake venom phosphodiesterase and 5 μl of 0.5 M Tris–HCl (pH 8.9). The digestion was continued at 37°C for 6 h and the enzymes were removed by chloroform extraction. The resulting aqueous solution was dried in a Speed-vac and redissolved in doubly distilled water for LC–MS/MS analysis.

ODN synthesis

ODNs were synthesized on a Beckman Oligo 1000S DNA synthesizer (Fullerton, CA, USA) at a 1-μmol scale. The synthesized phosphoramidite building blocks were dissolved in anhydrous acetonitrile at a concentration of 0.067 M. Standard phosphoramidite building blocks (Glen Research Inc., Sterling, VA, USA) of dA, dC, dG and dT were employed and a standard ODN assembly protocol was used without any modification. After synthesis, the ODN-bearing control pore glass (CPG) beads were first treated with 2.0 ml of 0.4 M NaOH at room temperature for 5 h and the beads were removed by filtration. The resulting ODN-containing solution was neutralized with 1.0 M HCl and the solvent was removed in a Speed-vac. The residue was then treated with concentrated NH_4OH (3.0 ml) at room temperature for 2 days and the solvent was removed by using Speed-vac. The dried pellet was reconstituted in water and purified by HPLC.

In an alternative ODN synthesis protocol, ultra-mild phosphoramidite building blocks of dA, dC and dG (Glen Research Inc., Sterling, VA, USA) were used. After synthesis, the ODN-bearing ultra-mild CPG beads were suspended in 0.4 M NaOH solution (3.0 ml) at room temperature for 5 h and the beads were subsequently removed by filtration. The resulting solution was neutralized with 1.0 M HCl and subjected to HPLC purification; HPLC Gradients I and II were used for purification of 12-mer and 20-mer ODNs, respectively (ODN sequences are shown in Table 1).

Enzymatic digestion of synthetic ODNs

A 20-μl solution containing 10 nmol of ODN1 or ODN2 was digested with four enzymes following the same procedures as described above for the digestion of KDA-treated calf thymus DNA. The resulting mixtures were subsequently subjected to HPLC analysis in which Gradient III was employed.

Table 1. Sequences of synthesized ODNs and the primer used for *in vitro* replication experiments

ODNs	Sequences[a]
ODN1/ODN2	5′-ATG GCG XGC TAT-3′
ODN3/ODN4	5′-ATG GCG XGC TAT GAT CCT AG-3′
Primer	5′-GCT AGG ATC ATA GC-3′

[a]In ODN1/ODN3, X = N^6-CMdA and in ODN2/ODN4, X = N^4-CMdC.

Thermodynamic studies

The lesion-bearing ODNs (ODN1 or ODN2) and their complementary strands were dissolved in a 1.1-ml solution containing NaCl (100 mM), sodium phosphate (10 mM, pH 7.0) and EDTA (50 μM) at a total ODN concentration (C_t) of 1.0, 2.0, 4.0, 8.0 or 16 μM. UV absorbance versus temperature profiles were recorded on a Varian Cary 500 spectrophotometer (Varian Inc.) in the reverse and forward directions for a temperature range of 80–10°C at the rate of 1.0°C/min, and the melting temperature (T_m) value was obtained by the derivative method. The thermodynamic parameters were obtained from the van't Hoff plot (27), in which the reciprocal of T_m was plotted against $\ln(C_t/4)$:

$$\frac{1}{T_m} = \frac{R}{\Delta H}\ln\frac{C_t}{4} + \frac{\Delta S}{\Delta H}$$

and equation:

$$\Delta G = \Delta H - T\Delta S$$

where R is the universal gas constant (1.987 cal $mol^{-1} K^{-1}$). The error limits for ΔG, ΔH and ΔS derived from fitted parameters were calculated by using the previously described equations (28,29).

In vitro replication studies with exonuclease-free Kf$^-$ of *Escherichia coli* DNA polymerase I

Primer extension experiments were carried out under standing-start conditions. The 20-mer lesion-containing templates and normal templates (50 nM) with dA or dC in lieu of N^6-CMdA or N^4-CMdC were annealed with a 5′-[^{32}P]-labeled 14-mer primer (50 nM), to which was added a mixture of all four dNTPs (100 μM each). The reaction was continued in a 10-μl solution containing 10 mM Tris–HCl (pH 7.5), 10 mM $MgCl_2$, 50 mM NaCl and 1 mM dithiothreitol (DTT) at 37°C for 30 min with different amounts of Kf$^-$ added (0, 0.05, 0.1, 0.2 and 0.3 U).

In vitro replication experiments were also performed in the presence of one type of dNTP at a time, where the concentration for individual dNTP was 1.0 mM and 0.1 U of Kf$^-$ was added. The reaction was continued at 37°C for 10 min and terminated by adding 8 μl of gel-loading buffer, which contained 80% formamide (pH 8.0), 10 mM EDTA and 1.0 mg/ml each of xylene cyanol and bromophenol. The products were resolved on 20% denaturing polyacrylamide gels containing 8 M urea. Gel images were obtained by using a Typhoon 9410 Variable Mode Imager (Amersham Biosciences Co.) and ImageQuant 5.2 software (Amersham Biosciences Co.).

RESULTS

Syntheses and structure characterization of N^6-CMdA and N^4-CMdC

Previous studies have shown that KDA is capable of inducing O^6-CMdG, $N3$-CMdT and O^4-CMdT in isolated DNA (11,18). It remains unexplored what types of adducts can be induced by KDA at adenine and cytosine sites in DNA. To examine the diazoacetate-induced carboxymethylation chemistry of adenine and cytosine, we first developed synthetic strategies for the preparation of N^6-CMdA and N^4-CMdC (Scheme 1). To this end, we introduced the ethoxycarbonylmethyl functionality to the N^6 position of 2′-deoxyadenosine by substitution of the chlorine atom in 6-CldA with glycine ethyl ester (30), and the resulting compound **1a** was hydrolyzed under alkaline conditions to render N^6-CMdA. N^4-CMdC was synthesized by using a nucleoside conversion strategy (26). In this context, the 1,2,4-triazolyl moiety in compound **2a** was replaced with glycine ethyl ester to render compound **2b**, which was hydrolyzed under similar alkaline conditions to yield the desired N^4-CMdC.

Identities of N^6-CMdA and N^4-CMdC were supported by ^{1}H NMR and HRMS measurements (see 'Materials and Methods' section). Moreover, we employed 2D heteronuclear multiple-bond correlation (HMBC) experiment to assign unambiguously the sites of carboxymethylation in these two modified nucleosides. In particular, the two methylene protons (at 3.96 p.p.m.) in the carboxymethyl functionality of the N^6-CMdA exhibit strong correlation with the carboxylic carbon atom, as well as the C6 atom (at 154 p.p.m.), but not the C2 atom, of the purine ring in a 2D HMBC spectrum (Supplementary Figure S10a). On the other hand, the corresponding methylene protons (at 3.86 p.p.m.) of the N^4-CMdC display strong correlation with the C4 atom (at 164 p.p.m.) of the pyrimidine ring and the carboxylic carbon (Supplementary Figure S10b). These distinct spectral features reveal without ambiguity the sites where the carboxymethyl moiety is introduced.

Formation of N^6-CMdA and N^4-CMdC in calf thymus DNA upon exposure to KDA

The availability of authentic N^6-CMdA and N^4-CMdC enabled us to assess whether these two lesions can be induced in DNA upon diazoacetate treatment. To this end, we treated calf thymus DNA with potassium diazoacetate, removed salts from the reaction mixture by ethanol precipitation, digested the DNA with enzymes and subjected the resulting nucleoside mixture to LC–MS/MS analysis, where we monitored selectively the fragmentation of the $[M+H]^+$ ions of the carboxymethylated derivatives of 2′-deoxyadenosine (m/z 310.1) and 2′-deoxycytidine (m/z 286.1). The selected-ion chromatograms (SICs; Figure 1) for monitoring the neutral loss of 2-deoxyribose (116 Da) from the protonated ions of the two carboxymethylated lesions revealed peaks at 30.5

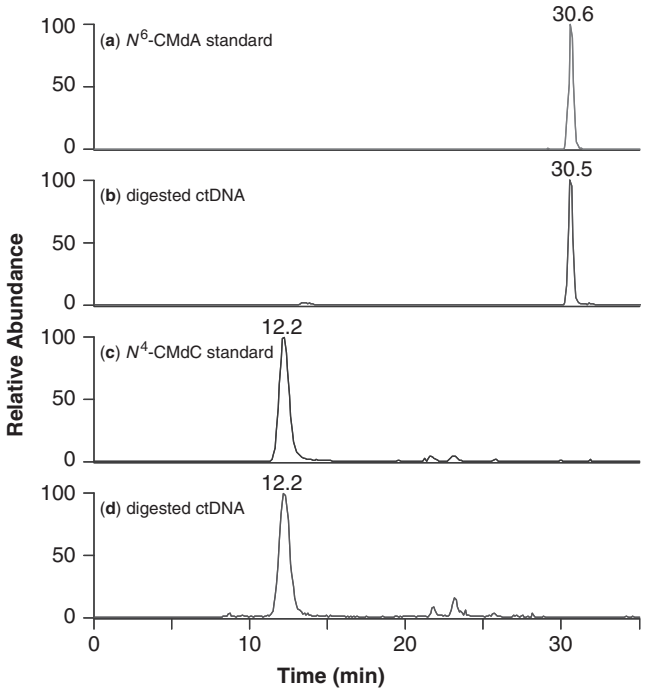

Figure 1. LC–MS/MS for monitoring the formation of N^6-CMdA and N^4-CMdC in KDA-treated calf thymus DNA. Shown are the SICs for monitoring the m/z 310.1→194.1 and 286.1→170.1 transition, corresponding to the loss of a 2-deoxyribose, from the LC–MS/MS analyses with the injection of: (**a**) N^6-CMdA standard; (**b**) enzymatic digestion mixture of calf thymus DNA treated with 10 mM of KDA; (**c**) N^4-CMdC standard; and (**d**) the same sample as in (b).

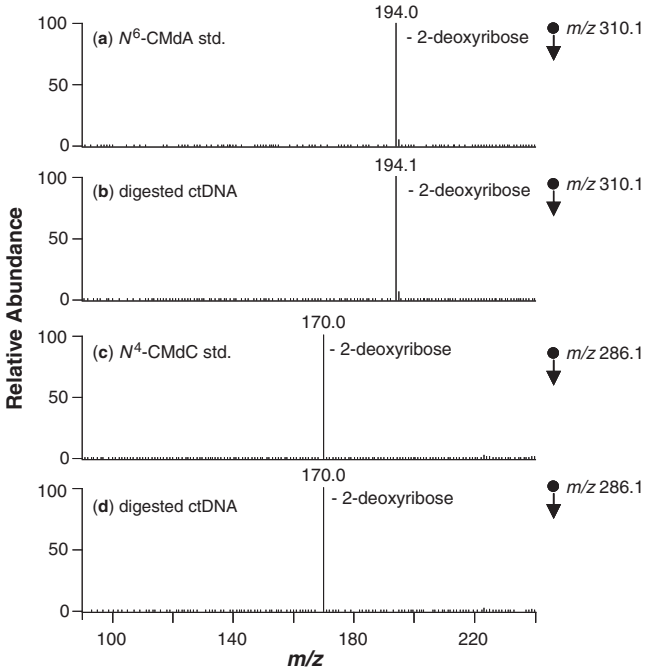

Figure 2. Collision-induced dissociation (CID) mass spectra supporting the formation of N^6-CMdA and N^4-CMdC in calf thymus DNA. Shown are the MS/MS results that monitor the fragmentation of the protonated-ions of N^6-CMdA (m/z 310.1) and N^4-CMdC (m/z 286.1), for: (**a**) standard N^6-CMdA; (**b**) the 30.5-min fraction shown in Figure 1b; (**c**) standard N^4-CMdC; and (**d**) the 12.2-min fraction shown in Figure 1d.

and 12.2 min, respectively (Figure 1b and d). The product-ion spectra averaged from these two peaks showed the formation of predominant fragment ions of m/z 194 and 170 for carboxymethylated 2′-deoxyadenosine and carboxymethylated 2′-deoxycytidine, respectively (Figure 2b and d), which are attributed to arise from the elimination of a 2-deoxyribose component.

We also subjected standard N^6-CMdA and N^4-CMdC to LC–MS/MS analysis under the same experimental conditions. It turned out that these two modified nucleosides share the same retention times (Figure 1a and c) and identical product-ion spectra (Figure 2a and c) as the two components present in the enzymatic digestion mixture of KDA-treated calf thymus DNA. This result demonstrated that N^6-CMdA and N^4-CMdC are the major carboxymethylated lesions of dA and dC, respectively, induced by KDA in calf thymus DNA.

Based on the peak areas found in the SICs for monitoring the neutral loss of 2-deoxyribose from the carboxymethylated derivatives of all four natural nucleosides and with the assumption that these carboxymethylated nucleosides exhibit the same ionization and fragmentation efficiencies, we estimated that the amount of N^6-CMdA was approximately 10 times greater than any other known carboxymethylated nucleosides (data not shown). In this context, we were also able to detect $N3$-CMdT, O^4-CMdT and O^6-CMdG in the same digestion mixture (18), and it is worth emphasizing that the accurate quantification of these lesions formed *in vitro* or in cells requires LC-MS/MS analysis with the use of stable isotope-labeled forms of the carboxymethylated nucleosides, and these compounds are currently being synthesized in our laboratory.

Solid-phase synthesis of ODNs containing site-specifically inserted N^6-CMdA and N^4-CMdC

Our experimental data clearly revealed that N^6-CMdA and N^4-CMdC can be induced in calf thymus DNA upon exposure to KDA, and ODNs bearing a site-specifically incorporated lesion are essential for future studies about how these lesions perturb DNA replication and how they are repaired. Therefore, we extended the above-described synthetic methods to the preparation of the phosphoramidite building blocks that allow for the insertion of N^6-CMdA and N^4-CMdC into ODNs by using automated solid-phase synthesis (Scheme 2). In this regard, it is worth noting that previous studies by Harris and coworkers (30) showed that ODNs containing some N^6-substituted dA derivatives could be obtained by nucleophilic displacements of chlorine atom in 6-CldA with amine-containing species. We attempted to employ a similar approach by incorporating 6-CldA into an ODN and treating the ODN with glycine or glycine ethyl ester; however, no appreciable displacement was observed after 3 days. Thus, we converted compound **1a** to its phosphoramidite building block (**1c**) and obtained the desired N^6-CMdA-bearing ODNs via post-oligomerization alkaline hydrolysis.

Likewise, we prepared the phosphoramidite building block for the methyl ester derivative of N^4-CMdC (compound **2e**) from compound **2b**. Removal of two hydroxyl groups in compound **2b** was carried out by treatment with 0.4 M TEA in methanol for one day, and in the mean time, the ethoxycarbonylmethyl moiety on C4 was converted to methoxycarbonylmethyl moiety (Scheme 2b). After this step, the phosphoramidite building block **2f** can be readily prepared following standard procedures.

We next incorporated the ester derivatives of N^6-CMdA and N^4-CMdC into ODNs. After synthesis, the ODN-bearing CPG beads were first treated with 0.4 M NaOH at room temperature for 5 h. Upon this treatment, the ester derivatives of the carboxymethyl functionality were hydrolyzed to the corresponding carboxylic acid, the ODNs were cleaved from the CPG beads and the nucleobase-protecting groups were partially removed. The complete deprotection of nucleobases was attained by further treatment with concentrated NH_4OH at room temperature for 2 days. It is worth noting that the above conversion/deprotection protocol is essential since direct treatment of the ester precursor-containing ODNs with concentrated NH_4OH, as used in standard ODN deprotection, gave rise to the facile conversion of the ester to its corresponding amide (data not shown).

We also developed an alternative ODN synthesis protocol where ultra-mild phosphoramidite building blocks were employed. Since the exocyclic amino groups of dA and dC are conjugated with ethoxy- and methoxycarbonylmethyl moieties, which simultaneously serve as nucleobase protecting groups, the phosphoramidite building blocks **1c** and **2e** can therefore be used directly for ODN assembly. After synthesis, a 5-h NaOH treatment is sufficient for cleavage, deprotection and ester-to-acid conversion. This strategy totally obviated the use of NH_4OH and it constituted an alternative protocol for the synthesis of ODNs bearing a carboxymethylated DNA adduct. The completely deprotected ODNs were then purified by HPLC and the HPLC traces are shown in supporting information (Supplementary Figures S11–S14).

ESI-MS and MS/MS characterizations of ODNs containing N^6-CMdA and N^4-CMdC

We next characterized the N^6-CMdA and N^4-CMdC-carrying ODNs by MS. Here, we use d(ATG GCG XGC TAT) (ODN1, 'X' represents N^6-CMdA) as an example to illustrate how we use ESI-MS and MS/MS to confirm the site of N^6-CMdA incorporation. Negative-ion ESI-MS analysis of this ODN gave a deconvoluted mass of 3741.8 Da for ODN1 (Figure 3a), which is 58 Da higher than the calculated mass of the unmodified d(ATG GCG AGC TAT) (i.e. 3683.8 Da). This result is consistent with the presence of an N^6-CMdA adduct in this substrate. The product-ion spectrum of the $[M\text{-}3H]^{3-}$ ion (m/z 1246.7) of ODN1 showed the formation of w_n ions (Figure 3b): w_3^-, w_4^-, w_5^-, w_6^-, w_5^{2-},w_6^{2-},w_7^{2-},w_8^{2-},w_9^{2-} and w_{11}^{3-}, as well as $[a_n$ - Base] ions: $[a_3 - G]^-$, $[a_4 - G]^-$, $[a_5 - C]^-$, $[a_6 - G]^-$, $[a_7 - X]^{2-}$, $[a_8 - G]^{2-}$, $[a_9 - C]^{2-}$ and $[a_{11} - A]^{2-}$ ions. The measured masses for the w_3, w_4 and w_5 ions were the same as the calculated masses for the corresponding ions of the unmodified ODN, whereas the w_6, w_7, w_8, w_9 and w_{11} ions exhibited 58 Da higher in mass than the corresponding fragment ions formed from the unmodified ODN. These results are consistent with the presence of an N^6-CMdA at the seventh position in the ODN. The above finding is further supported by the observed masses for the $[a_n$ - Base] ions. In this respect, the measured masses for the $[a_8$- G], $[a_9$- C] and $[a_{11}$- A] ions are 58 Da higher, whereas the measured masses of the $[a_3$ - G], $[a_4$ - G], $[a_5$ - C], $[a_6$ - G] and $[a_7$- X] ions are the same as the calculated ones of the corresponding fragment ions for the unmodified d(ATG GCG AGC TAT). The other sequences were also confirmed by the similar ESI-MS and MS/MS analyses (Supplementary Figures S15–S17).

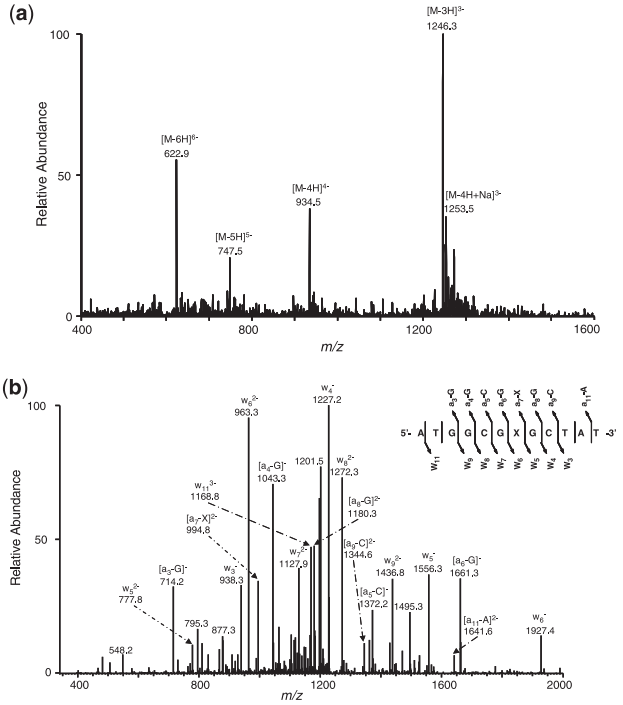

Figure 3. ESI-MS and MS/MS characterizations of d(ATGGCGXGCTAT), X = N^6-CMdA: (**a**) negative-ion ESI-MS; (**b**) product-ion spectrum of the $[M\text{-}3H]^{3-}$ ion (m/z 1246.3).

Homogeneity of the lesion-containing ODNs

To further confirm the incorporation of N^6-CMdA and N^4-CMdC into ODNs, we digested ODN1 and ODN2 into 2′-deoxynucleosides, separated the digestion mixtures by HPLC and verified each component by ESI-MS. Indeed, the HPLC traces revealed the presence of N^6-CMdA in the digestion mixture of ODN1 (the 25.4 min fraction; Supplementary Figure S18a) and N^4-CMdC in the digestion mixture of ODN2 (the 12.6 min fraction; Supplementary Figure S18b).

We further integrated the peak areas of dC, dT, dG and N^6-CMdA or N^4-CMdC in HPLC traces; peak area of dA was not estimated due to the partial deamination of dA to

Table 2. Thermodynamic parameters for duplex formation

Duplex	ΔH (kcal mol^{-1})	ΔS (cal mol^{-1} K^{-1})	$\Delta G_{25^\circ C}$ (kcal mol^{-1})	$\Delta\Delta G_{25^\circ C}$ (kcal mol^{-1})
5′-ATGGCGXGCTAT-3′				
3′-TACCGCTCGATA-5′				
X = dA	−101.4 ± 3.3	−286 ± 14	−16.1 ± 0.4	
X = N^6-CMdA	−76.7 ± 2.1	−221 ± 7	−10.8 ± 0.2	5.3
5′-ATGGCGXGCTAT-3′				
3′-TACCGCGCGATA-5′				
X = dC	−119.0 ± 3.8	−333 ± 16	−19.7 ± 0.5	
X = N^4-CMdC	−78.5 ± 2.5	−220 ± 7	−12.9 ± 0.2	6.8

$\Delta\Delta G_{25^\circ C}$ = $\Delta G_{25^\circ C}$ (lesion-containing duplex) − $\Delta G_{25^\circ C}$ (unmodified duplex).

2′-deoxyinosine induced by residual adenosine deaminase present in the commercial preparation of the enzyme(s) used in DNA digestion. With the consideration of the molar extinction coefficients of nucleosides at 260 nm [i.e. 12 100 L mol^{-1} cm^{-1} and 9300 L mol^{-1} cm^{-1} were found for N^6-CMdA and N^4-CMdC by using a previously described method (31)], the molar ratio of N^6-CMdA:dC:dT:dG turned out to be 1.0:2.1:3.1:4.2 for ODN1, and the molar ratio of N^4-CMdC:dC:dT:dG for ODN2 was 1.0:2.0:3.0:4.0. These data are consistent with the presence of one N^6-CMdA or N^4-CMdC, two dC, three dT and four dG residues in the two ODNs.

Thermodynamic properties of lesion-containing DNA duplexes

To examine how the presence of N^6-CMdA and N^4-CMdC affects duplex stability, we determined the thermodynamic parameters for the formation of duplex DNA harboring an N^6-CMdA, N^4-CMdC, or unmodified dA and dC by melting temperature measurements. The ODN sequences used in this study were ODN1 and ODN2 (Table 1), and the ΔH and ΔS were calculated from the intercept and slope found in the van't Hoff plot following the equations described in the 'Materials and Methods' section (Supplementary Figure S19). It turned out that the presence of N^6-CMdA and N^4-CMdC destabilized the duplex by 5.3 and 6.8 kcal/mol in free energy at 25°C, respectively (Table 2).

In vitro replication studies with Kf$^-$

We next examined the bypass of N^6-CMdA and N^4-CMdC with the Kf$^-$ by carrying out *in vitro* primer extension assays. To this end, we assessed the ability of the Kf$^-$ that has been used extensively as a model replicative polymerase, to extend a 5′-[^{32}P]-labeled 14-mer primer annealed with the N^6-CMdA- or N^4-CMdC-bearing 20-mer template in the presence of all four dNTPs. The primer extension results unveiled that N^6-CMdA does not block substantially the DNA synthesis mediated by Kf$^-$ and the full-length products can be readily detected. N^4-CMdC, however, inhibits markedly the DNA synthesis, though a small amount of full-length products could also be detected. In both cases, synthesis did not stop after the incorporation of one nucleotide opposite N^6-CMdA or N^4-CMdC (Figure 4a). When the above primer/template complex was incubated with Kf$^-$ in the presence of one type of nucleotide at a time, we found that the correct nucleotides, dT and dG, are preferentially incorporated opposite N^6-CMdA and N^4-CMdC, respectively. However, misincorporation also occurred, that is, Kf$^-$ incorporates dAMP opposite N^6-CMdA, and dTMP or dAMP opposite N^4-CMdC (Figure 4b).

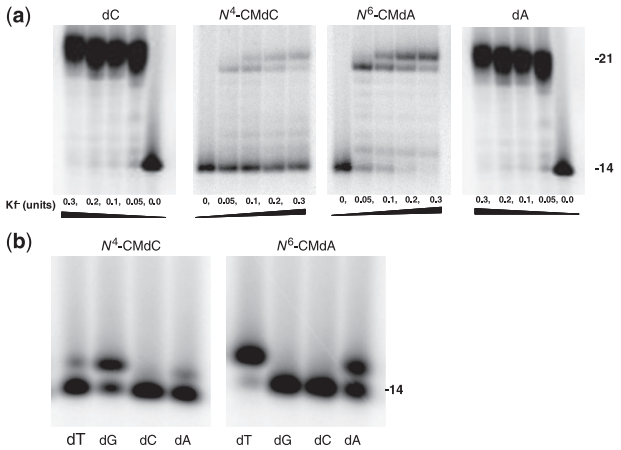

Figure 4. *In vitro* replication studies of N^6-CMdA- or N^4-CMdC-bearing ODNs and the corresponding unmodified substrates with Kf$^-$ of *E. coli* DNA polymerase I. A template, d(ATGGCGXGCTATGATCCTAG) ('X' represents N^6-CMdA, N^4-CMdC, dA or dC), and a 5′-[^{32}P]-labeled primer, d(p*GCTAGGATCATAGC), were employed. The concentration of the resulting duplex ODNs was 50 nM. The replication experiments were carried out: (**a**) in the presence of all four dNTPs at a concentration of 1.0 mM each for 30 min and the amounts of Kf$^-$ are indicated in the figure; and (**b**) in the presence of dNTPs individually ([dNTP] = 1.0 mM) at 37°C for 10 min, and 0.1 U of Kf$^-$ was used.

DISCUSSION

Recently, emerging data have shown that exposure to NOCs and the resultant carboxymethylation of DNA are significantly associated with the risk of developing non-cardia gastric cancer (2,32). Some earlier studies (11) along with recent results from our laboratory (18) suggested that all four nucleosides can be carboxymethylated, with the highest yield being observed for N^6-CMdA (*vide supra*). Obtaining ODNs bearing a

site-specifically incorporated carboxymethylated lesion constitutes a crucial step toward examining the biological implications of the lesion at the molecular level. Syntheses of O^6-CMdG-, $N3$-CMdT- and O^4-CMdT-containing ODNs were reported previously (12,18). In this study, we developed facile synthetic strategies for the preparation of authentic N^6-CMdA and N^4-CMdC, as well as the phosphoramidite building blocks of their ester derivatives. The latter compounds facilitate the incorporation of N^6-CMdA and N^4-CMdC into ODNs at defined sites. We demonstrated that the method allowed for the preparation of 12- and 20-mer ODNs in reasonably good yield. We were able to obtain ~200 nmol of the lesion-bearing ODNs from a 1-μmol scale synthesis. Together with previously published synthetic strategy for O^6-CMdG (12,25), $N3$-CMdT and O^4-CMdT (18), it can be concluded that the ester derivatives of carboxymethyl moieties are universal precursors for the syntheses of phosphoramidite building blocks for the preparation of ODNs containing site-specifically inserted carboxymethylated DNA lesions. Additionally, the alkaline conditions for the conversion from ester to acid after oligomerization are compatible with ODN deprotection protocols.

Thermodynamic parameters for duplex formation, as derived from melting temperature measurements, revealed that the introduction of an N^6-CMdA and N^4-CMdC into duplex DNA led to an increase in ΔG for duplex formation at 25°C by 5.3 and 6.8 kcal/mol, respectively (Table 2). The increases in ΔG for duplex formation are much larger than what we observed for N^2-(1-carboxyethyl)-2′-deoxyguanosine (3.8 and 4.0 kcal/mol for the S and R diastereomers, respectively) (33). The destabilization to a DNA double helix induced by N^6-CMdA and N^4-CMdC might occur through a significant change to local DNA structures. Additionally, the presence of the carboxymethyl functionality at the N^6 position of adenine and the N^4 position of cytosine may perturb the tautomeric equilibrium of these nucleobases thereby destabilizing duplex DNA. Future structural studies of N^6-CMdA- and N^4-CMdC-bearing duplex DNA will offer important insights into the substantial destabilization of duplex DNA introduced by these two lesions.

The primer extension results unveiled that N^6-CMdA does not block significantly the DNA synthesis across the lesion site mediated by Kf$^-$ and full-length products can be detected at a relatively high percentage. N^4-CMdC, however, blocked remarkably the DNA synthesis across the lesion site although there was a small amount of full-length products. These results are consistent with previous studies showing that Kf$^-$ could bypass other N^6-dA adducts induced by styrene oxide or benzo[*a*]pyrene-7,8-dihydrodiol-9,10-epoxide (34,35), whereas little is known about how Kf$^-$ bypasses N^4-dC adducts.

When the *in vitro* replication with Kf$^-$ was first carried out in the presence of one type of nucleotide at a time, we found that, aside from correct nucleotide insertion, Kf$^-$ incorporated readily the wrong nucleotides, dAMP, opposite N^6-CMdA, and the enzyme also induced the misinsertion of dAMP and dTMP opposite N^4-CMdC. This finding is consistent with results from a previous shuttle vector study showing that KDA induces GC→TA and AT→TA transversions and GC→AT transitions in a *p53* gene (17). Future steady-state kinetic measurements for nucleotide incorporation opposite and beyond the lesion sites and studies on how N^6-CMdA and N^4-CMdC perturb DNA replication *in vivo* will afford more insights into the biological implications of these carboxymethylated lesions, and the availabilities of the lesion-containing substrates render such studies possible.

Some initial repair studies have been carried out for O^6-CMdG, and it was found that the azaserine-mediated cell killing cannot be rescued by the overexpression of O^6-methylguanine methyltransferase (MGMT) (36), which is in line with the observation that O^6-CMdG is not subjected to repair by MGMT *in vitro* (11). On the other hand, lymphoblastoid cells deficient in nucleotide excision repair (NER) were significantly more sensitive to azaserine than the control repair-proficient cells, suggesting that some azaserine-induced DNA lesions can be repaired by NER factors (36). The availability of the N^6-CMdA- and N^4-CMdC-carrying substrates also facilitates the future investigations about how these lesions are repaired.

SUPPLEMENTARY DATA

Supplementary Data are available at NAR Online.

FUNDING

National Institutes of Health (R01 DK082779). Funding for open access charge: R01 DK082779.

Conflict of interest statement. None declared.

REFERENCES

1. Lindahl,T. (1993) Instability and decay of the primary structure of DNA. *Nature*, **362**, 709–715.
2. Correa,P. (1992) Human gastric carcinogenesis: a multistep and multifactorial process - 1st American Cancer Society award lecture on cancer epidemiology and prevention. *Cancer Res.*, **52**, 6735–6740.
3. Tricker,A.R. (1997) *N*-nitroso compounds and man: sources of exposure, endogenous formation and occurrence in body fluids. *Eur. J. Cancer Prev.*, **6**, 226–268.
4. Risch,H.A. (2003) Etiology of pancreatic cancer, with a hypothesis concerning the role of *N*-nitroso compounds and excess gastric acidity. *J. Natl Cancer Inst.*, **95**, 948–960.
5. Hecht,S.S. (1999) DNA adduct formation from tobacco-specific *N*-nitrosamines. *Mutat. Res.*, **424**, 127–142.
6. Kokkinakis,D.M. and Subbarao,V. (1993) The significance of DNA damage, its repair and cell proliferation during carcinogen treatment in the initiation of pancreatic cancer in the hamster model. *Cancer Res.*, **53**, 2790–2795.
7. Howatson,A.G. and Carter,D.C. (1987) Pancreatic carcinogenesis: effect of secretin in the hamster- nitrosamine model. *J. Natl Cancer Inst.*, **78**, 101–105.
8. Busby,W.F. Jr, Shuker,D.E., Charnley,G., Newberne,P.M., Tannenbaum,S.R. and Wogan,G.N. (1985) Carcinogenicity in rats of the nitrosated bile acid conjugates *N*-nitrosoglycocholic acid and *N*-nitrosotaurocholic acid. *Cancer Res.*, **45**, 1367–1371.
9. Puju,S., Shuker,D.E., Bishop,W.W., Falchuk,K.R., Tannenbaum,S.R. and Thilly,W.G. (1982) Mutagenicity of

N-nitroso bile acid conjugates in Salmonella typhimurium and diploid human lymphoblasts. *Cancer Res.*, **42**, 2601–2604.
10. Shuker,D.E.G., Tannenbaum,S.R. and Wishnok,J.S. (1981) *N*-Nitroso bile-acid conjugates. 1. synthesis, chemical reactivity, and mutagenic activity. *J. Org. Chem.*, **46**, 2092–2096.
11. Shuker,D.E.G. and Margison,G.P. (1997) Nitrosated glycine derivatives as a potential source of O^6-methylguanine in DNA. *Cancer Res.*, **57**, 366–369.
12. Harrison,K.L., Fairhurst,N., Challis,B.C. and Shuker,D.E.G. (1997) Synthesis, characterization and immunochemical detection of O^6-carboxymethyl-2′-deoxyguanosine: a DNA adduct formed by nitrosated glycine derivatives. *Chem. Res. Toxicol.*, **10**, 652–659.
13. Harrison,K.L., Jukes,R., Cooper,D.P. and Shuker,D.E.G. (1999) Detection of concomitant formation of O^6-carboxymethyl- and O^6-methyl-2′-deoxyguanosine in DNA exposed to nitrosated glycine derivatives using a combined immunoaffinity/HPLC method. *Chem. Res. Toxicol.*, **12**, 106–111.
14. Cupid,B.C., Zeng,Z.T., Singh,R. and Shuker,D.E.G. (2004) Detection of O^6-carboxymethyl-2′-deoxyguanosine in DNA following reaction of nitric oxide with glycine and in human blood DNA using a quantitative immunoslot blot assay. *Chem. Res. Toxicol.*, **17**, 294–300.
15. Longnecker,D.S. and Curphey,T.J. (1975) Adenocarcinoma of the pancreas in azaserine-treated rats. *Cancer Res.*, **35**, 2249–2258.
16. Zurlo,J., Curphey,T.J., Hiley,R. and Longnecker,D.S. (1982) Identification of 7-carboxymethylguanine in DNA from pancreatic acinar cells exposed to azaserine. *Cancer Res.*, **42**, 1286–1288.
17. Gottschalg,E., Scott,G.B., Burns,P.A. and Shuker,D.E.G. (2007) Potassium diazoacetate-induced *p*53 mutations in vitro in relation to formation of O^6-carboxymethyl- and O^6-methyl-2′-deoxyguanosine DNA adducts: relevance for gastrointestinal cancer. *Carcinogenesis*, **28**, 356–362.
18. Wang,J. and Wang,Y. (2009) Chemical synthesis of oligodeoxyribonucleotides containing *N*3- and O^4-carboxymethylthymidine and their formation in DNA. *Nucleic Acids Res.*, **37**, 336–345.
19. Wood,D.J., Hruska,F.E. and Ogilvie,K.K. (1974) Proton magnetic resonance studies of 2′-deoxythymidine, its 3′- and 5′-monophosphates and 2′-deoxythymidylyl-(3′,5′)-2′-deoxythymidine in aqueous solution. *Can. J. Chem.*, **52**, 3353–3366.
20. van der Wenden,E.M., von Frijtag Drabbe Kunzel,J.K., Mathot,R.A.A., Danhof,M., IJzerman,A.P. and Soudijn,W. (1995) Ribose-modified adenosine analogues as potential partial agonists for the adenosine receptor. *J. Med. Chem.*, **38**, 4000–4006.
21. Ikejiri,M., Saijo,M., Morikawa,S., Fukushi,S., Mizutani,T., Kurane,I. and Maruyama,T. (2007) Synthesis and biological evaluation of nucleoside analogues having 6-chloropurine as anti-SARS-CoV agents. *Bioorg. Med. Chem. Lett.*, **17**, 2470–2473.
22. Braibante,M.E.F., Braibante,H.T.S., Morel,A.F., Costa,C.C. and Lima,M.G. (2006) The solvent free preparation of b-amino esters a,b-unsaturated ketones and esters with domestic microwave oven. *J. Braz. Chem. Soc.*, **17**, 184–188.
23. Clive,D.L.J., Hisaindee,S. and Coltart,D.M. (2003) Derivatized amino acids relevant to native peptide synthesis by chemical ligation and acyl transfer. *J. Org. Chem.*, **68**, 9247–9254.
24. Gao,Y., Zhang,P., Wu,L., Matsuura,T. and Meng,J.B. (2003) Synthesis of uridine derivatives containing amino acid residues. *Synth. Commun.*, **33**, 2635–2641.
25. Xu,Y.Z. (2000) Synthesis and characterization of DNA containing O^6-carboxymethylguanine. *Tetrahedron*, **56**, 6075–6081.
26. Xu,Y.Z. and Swann,P.F. (1990) A simple method for the solid phase synthesis of oligodeoxynucleotides containing O^4-alkylthymine. *Nucleic Acids Res.*, **18**, 4061–4065.
27. Breslauer,K.J. (1995) Extracting thermodynamic data from equilibrium melting curves for oligonucleotide order-disorder transitions. *Meth. Enzymol.*, **259**, 221–242.
28. Persmark,M. and Guengerich,F.P. (1994) Spectroscopic and thermodynamic characterization of the interaction of N^7-guanyl thioether derivatives of d(TGCTG*CAAG) with potential complements. *Biochemistry*, **33**, 8662–8672.
29. Santalucia,J., Kierzek,R. and Turner,D.H. (1991) Functional-group substitutions as probes of hydrogen-bonding between GA mismatches in RNA internal loops. *J. Am. Chem. Soc.*, **113**, 4313–4322.
30. Harris,C.M., Zhou,L., Strand,E.A. and Harris,T.M. (1991) New strategy for the synthesis of oligodeoxynucleotides bearing adducts at exocyclic amino sites of purine nucleosides. *J. Am. Chem. Soc.*, **113**, 4328–4329.
31. Hong,H. and Wang,Y. (2005) Formation of intrastrand cross-link products between cytosine and adenine from UV irradiation of d(^{Br}CA) and duplex DNA containing a 5-bromocytosine. *J. Am. Chem. Soc.*, **127**, 13969–13977.
32. Jakszyn,P., Bingham,S., Pera,G., Agudo,A., Luben,R., Welch,A., Boeing,H., Del Giudice,G., Palli,D., Saieva,C. *et al.* (2006) Endogenous versus exogenous exposure to *N*-nitroso compounds and gastric cancer risk in the European Prospective Investigation into Cancer and Nutrition (EPIC-EURGAST) study. *Carcinogenesis*, **27**, 1497–1501.
33. Cao,H., Jiang,Y. and Wang,Y. (2007) Stereospecific synthesis and characterization of oligodeoxyribonucleotides containing an N^2-(1-carboxyethyl)-2′-deoxyguanosine. *J. Am. Chem. Soc.*, **129**, 12123–12130.
34. Chary,P. and Lloyd,R.S. (1995) In-vitro replication by prokaryotic and eukaryotic polymerases on DNA templates containing site-specific and stereospecific benzo[a]pyrene-7,8-dihydrodiol-9,10-epoxide adducts. *Nucleic Acids Res.*, **23**, 1398–1405.
35. Latham,G.J., Harris,C.M., Harris,T.M. and Lloyd,R.S. (1995) The efficiency of translesion synthesis past single styrene oxide DNA-adducts in-vitro is polymerase-specific. *Chem. Res. Toxicol.*, **8**, 422–430.
36. O'Driscoll,M., Macpherson,P., Xu,Y.Z. and Karran,P. (1999) The cytotoxicity of DNA carboxymethylation and methylation by the model carboxymethylating agent azaserine in human cells. *Carcinogenesis*, **20**, 1855–1862.